

# Timing and Spectral Properties of X-ray Emission from the Converging Flows onto Black hole: Monte-Carlo Simulations

Philippe Laurent<sup>1</sup>, Lev Titarchuk<sup>1,2,3</sup>

## ABSTRACT

We demonstrate that a X-ray spectrum of a converging inflow (CI) onto a black hole is the sum of a thermal (disk) component and the convolution of some fraction of this component with the Comptonization spread (Green's) function. The latter component is seen as an extended power law at energies much higher than the characteristic energy of the soft photons. We show that the high energy photon production (source function) in the CI atmosphere is distributed with the characteristic maximum at about the photon bending radius,  $1.5r_s$ , independently of the seed (soft) photon distribution. We show that high frequency oscillations of the soft photon source in this region lead to the oscillations of the high energy part of the spectrum but not of the thermal component. The high frequency oscillations of the inner region are not significant in the thermal component of the spectrum. We further demonstrate that Doppler and recoil effects (which are responsible for the formation of the CI spectrum) are related to the hard (positive) and soft (negative) time lags between the soft and hard photon energy channels respectively.

Subject headings: black hole physics | accretion disks | radiation mechanisms:  
nonthermal | X-rays: general

## 1. Introduction

Accreting stellar-mass black holes (BH) in Galactic binaries exhibit so called high-soft and low-hard spectral states (e.g. Borozdin et al. 1999, hereafter BOR99). An increase

---

<sup>1</sup>CEA, DSM/DAPNIA/SAP, Centre d'Etudes de Saclay, 91191 Gif-sur-Yvette Cedex, France; plau-  
rent@cea.fr

<sup>2</sup>George Mason University/Center for Earth Observing and Space Research, Fairfax VA 22030-4444;

<sup>3</sup>US Naval Research Laboratory, Space Science Division, 4555 Overlook Avenue, SW, Washington, DC  
20375-5352; lev@xip.nrl.navy.mil

in the soft blackbody luminosity component leads to the appearance of an extended power law. An important observational fact is that this effect is seen as a persistent phenomenon only in BH candidates, and thus it is apparently a unique black hole signature. Although in Neutron star (NS) systems similar power law components are detected in the intermediate stages (Strickman & Barret 1999; Iaria et al. 2000; DiSalvo et al. 2001), they are of a transient nature, disappearing with increasing luminosity (DiSalvo et al.).

It thus seems a reasonable assumption that the unique spectral signature of the soft state of BH binaries is directly tied to the black hole event horizon. This is the primary motivation for the Bulk Motion Comptonization Model (BMC) introduced in several previous papers, and recently applied with striking success to a substantial body of observational data (Shrader & Titarchuk 1998; BOR99; Titarchuk & Shrader 2002, hereafter TS02). A complete theory of BH accretion must, however, be also able to accommodate in a natural manner a growing number of observational traits exhibited in the temporal domain. For example, it is now well established that BH X-ray binaries exhibit quasi-periodic oscillation (QPO) phenomena in three frequency domains:  $0.1$  Hz,  $(1 - 10)$  Hz and  $(10^3 - 10^4)$  Hz. The

$10^3 - 10^4$  Hz QPOs seem to occur during periods of  $\alpha$ -ring, and when the spectra (although in the high-soft state) tend to be relatively hard, i.e. the relative importance of the power-law component with respect to the thermal. Furthermore, the QPO amplitudes increase with energy, that is there is a higher degree of modulation of the signal in the hard-power law than in the thermal excess component. In addition to the QPO phenomena, it has been noted by Nowak et al. (2000) (also see Cui et al. 2000) that measures of the coherence between the intensity variations in the hard power law and thermal components is negligible.

We argue that the BH X-ray spectrum in the high-soft state is formed in the relatively cold accretion flow with a subrelativistic bulk velocity  $v_{\text{bulk}} \ll c$  and with a temperature of a few keV and less ( $v_{\text{th}} \ll c$ ). In such a flow the effect of the bulk Comptonization is much stronger than the effect of the thermal Comptonization which is a second order with respect to  $v_{\text{th}} = c$ . In this Letter we present results of Monte Carlo simulations probing the spatial, spectral, timing and time-lag properties of X-ray radiation in CI atmosphere in xx2-4. Comparisons are drawn to the recent X-ray observations of BH sources. Summary and conclusions follow in x5.

## 2. Emergent spectrum and hard photon spatial distribution

The geometry used in these simulations is similar to the one used in the Laurent & Titarchuk (1999), hereafter LT99, consisting of a thin disk with an inner radius of  $3 r_s$ , merged with a spherical CI cloud harboring a BH in its center, where  $r_s = 2GM/c^2$  is the

Schwarzschild radius and  $M$  is a BH mass. The cloud outer radius is  $r_{\text{out}}$ . The disk is assumed always to be optically thick.

In addition to free-fall into the central BH, we have also taken into account the thermal motion of the CI electrons, simulated at an electron temperature of 5 keV. This is likely to be a typical temperature of the CI in the high-soft state of galactic BHs [see Chakrabarti & Titarchuk (1995) and BOR 99 for details]. The seed X-ray photons were generated uniformly and isotropically at the surface of the border of the accretion disk, from  $r_{\text{d,in}} = 3r_s$  to  $r_{\text{d,out}} = 10r_s$ . These photons were generated according to a thermal spectrum with a single temperature of 0.9 keV, similar to the ones measured in Black Hole binary systems (see for example BOR 99). In fact, BOR 99 also demonstrate that the multicolor disk spectrum can be fitted by the effective single temperature blackbody spectrum in the energy range of interest (for photon energies higher than 2 keV). The parameters of our simulations are the BH mass  $m$  in solar units, the CI electron temperature,  $T_e = 5\text{keV}$ , the mass accretion rate,  $\dot{m} = 4$  in Eddington units (see LT 99), and the cloud outer radius,  $r_{\text{out}} = 10r_s$ . It is worth noting that, for these parameters, the bulk motion effects are not significant at  $r > 10r_s$ .<sup>4</sup>

In Figure 1 we present the simulated spectrum of the X-ray emission emerging from the CI atmosphere. The spectrum exhibits three features: a soft X-ray bump, an extended power law and a sharp exponential turnover near 300 keV. As demonstrated previously (Titarchuk & Zannias 1998, hereafter TZ98; LT 99) the extended power law is a result of soft photon upscattering off CI electrons. The qualitative explanation of this phenomena was given by Ebisawa et al. (1996), hereafter ETC and later by Papathanassiou & Psaltis (2001). The exponential turnover is formed by a small fraction of those photons which undergo scatterings near the horizon where the strong curvature of the photon trajectories prevent us from detecting most of them. In Figure 1 we indicate, with arrows the places in the CI atmosphere where photons of a particular energy mainly come from.<sup>5</sup>

A precise analysis of the X-ray photon distribution in CI atmosphere can be made through calculation of the source function, either by semi-analytical methods solving the relativistic kinetic equation (RKE) (TZ98) or by Monte Carlo simulations (LT 99). TZ98 calculate the photon kinetics in the lab frame demonstrating that the source function has a strong peak near the photon bending radius,  $1.5r_s$  (Fig. 3 there). In Figure 2 we show the

---

<sup>4</sup>In general, the bulk motion Comptonization is effective when  $v_{\text{bulk}}/c = \dot{m}/r_s$  is not smaller than unity (e.g. Rees, 1978; Titarchuk et al. 1997).

<sup>5</sup>Recently, Reig et al. (2001) show that the extended power law can be also formed as a result of the bulk motion Comptonization when the rotational component is dominant in the flow. The photons gain energy from the rotational motion of the electrons.

Monte Carlo simulated source functions for four energy bands: 2–5 keV (curve a), 5–13 keV (curve b), 19–29 keV (curve c) and 60–150 keV (curve d). The peak at around  $(1.5 \pm 0.2)r_g$  is clearly seen for the second and the third bands which is in a good agreement with TZ98's source function.<sup>6</sup>

TZ98 calculated the upscattering part of spectrum neglecting the recoil effect. Our Monte Carlo simulations, not limited by TZ98's approximation, reproduce the source function spatial distribution for high energy bands (curve d in Figure 2). We confirm that the density of the highest energy X-ray photons is concentrated near the black hole horizon. Comparison of TZ98's semi-analytical calculations and our Monte-Carlo simulations leads us to conclude that the source function really follows the RKE first eigenfunction distribution until very high energies. At that point the upscattering photon spatial distribution also becomes a function of energy. As seen from Figure 2 the source function in the soft energy band (curve a) has two maxima: one is at  $2.2 r_g$  related to the photon bending radius and another (wide one) is at  $5 r_g$  affected by the disk emission area.

### 3. An Illumination Effect of C I Atmosphere and High Frequency QPO Phenomena

We remind the reader that the emergent spectrum is a result of integration of the product of the photon escape probability and the source function distribution along a line of sight (e.g. Chandrasekhar 1960). The normalization of the upscattering spectrum is determined by the fraction of the soft (disk) photons which illuminate the inner region of the C I atmosphere below  $3r_g$ , i.e. around the maximum of the upscattered photon source function. From the Monte Carlo simulations we extract the fraction of the soft photons emitted at some particular disk radius  $r$  which form the high energy part of spectrum (for  $E > 10$  keV). This distribution is presented in the upper panel of Figure 3. As seen from this plot, the strength of the high energy tail is mostly determined by the photons emitted at the inner edge of the disk. Thus any perturbation in the disk should be immediately translated to the oscillation of the hard tail with a frequency related to the inner disk edge. The C I atmosphere manifests the high frequencies QPO of the innermost part of the disk. In the lower panel of Figure 3 we present the power density spectrum for the simulated X-ray emission coming from C I atmosphere in the energies higher than 10 keV. We assume that

---

<sup>6</sup>TZ98 implemented the method of separation of variables to solve the RKE Green's function. They then showed that the source function of the upscattered photons is distributed according to the first eigenfunction of the RKE space operator defined by equations (21-24) in TZ98.

the PDS is a sum of the red noise component (where the power law index equals to 1) and QPOs power proportional to the illumination factor for a given disk radius,  $r$  (see the upper panel). We also assume that the perturbation frequency at  $r$  is related to the Keplerian frequency  $\nu_K = 2.2(3r_g=r)^{1.5} \text{ m kHz}$ .

There is a striking similarity between the high frequency QPO and spectral energy distribution of the Monte Carlo results and real observations of BHC in their soft-high state. For example, in XTE J1550-564 the 200 Hz QPO phenomenon tends to be detected in the high state at times when the bolometric luminosity surges and the hard-power-law spectral component is prominent (TS02). The noted lack of coherence between intensity variations of the high-soft-state low energy bands is also in a good agreement with our simulations where the high energy tail intensity correlates with the supply of the soft photons from the inner disk edge but it does not correlate with the production of the disk photons at large.

#### 4. Positive and Negative Time Lags

Additional important information related to the X-ray spectral-energy distribution can be extracted from the time lags between different energy bands. The hard and soft lags have been observed for several sources (e.g. Reig et al. 2000, hereafter R00; Tomack & Kaaret 2000 for GRS 1915+105 and Wijhards et al. 1999, Remillard et al. 2001 for XTE J1550-564). It is natural to expect the positive time lags in the case of the unsaturated thermal Comptonization. The primary soft photons gain energy in process of scattering off hot electrons; thus the hard photons spend more time in the cloud than the soft ones. Nobili et al. (2000) first suggested that in a corona with a temperature stratification (a hot core and a relatively cold outer part) the thermal Comptonization can account for the positive and negative time lags as well as the observed colors (see R00).<sup>7</sup>

In the bulk-motion Comptonization case, the soft disk photons at first gain energy in the deep layers of the converging inflow, and then in their subsequent path towards the observer lose energy in the relatively cold outer layers. If the overall optical depth of the converging inflow atmosphere (or the mass accretion rate) is near unity, we would detect only the positive lags as in the thermal Comptonization case, because relatively few photons would lose energy in escaping. But with an increase of the optical depth, the soft lags appear because more hard photons lose their energy in the cold outer layers.

---

<sup>7</sup>This Comptonization model with a hot core (for the similar models, see also Skibo & Demer 1995 and Lehr et al. 2000) may reproduce the intrinsic spectral and timing properties of the converging inflow.

In Figure 4 we present the calculations of the of time lags for two energy bands 2-13 keV and 13-900 keV. We first compute the time spent by the photon, drawn in a given direction, to cross the whole system without being scattered. Then, we compute the real time of flight of the photon, taking into account its scattering and its complete trajectory in the system. The general relativistic gravitational time dilatation was also taken into account in these computations. The time lag is then determined as a difference between these two times. In this time-lag definition, a photon which undergoes no scattering has a zero lag. Thus the time lags between two energy bands can be defined as a difference of these two time lags, i.e.  $\tau = \tau_2 - \tau_1$  where  $\tau_1$  and  $\tau_2$  are time lags for 2-13-keV and 13-900-keV bands respectively. The time lags for 2-13-keV band are distributed over the interval between 1 and 600 Schwarzschild times,  $t_s = r_s/c$  and the time lags for 13-900-keV band are distributed over the interval between 200 and  $10^3 t_s$ . For a ten solar mass BH  $t_s = 0.1$  m s. Thus, for  $\tau_1 < 15$  m s all time lags  $\tau$  are positive, i.e. high energy photons are produced later than the soft energies photons. The  $\tau_2$  distribution has a broad peak at 30 m s and  $\tau_1$  distribution has a broad peak at 8 m s. Consequently, the positive lags  $\tau$  are mostly higher than 20 m s. which is in a good agreement with the time lags detection in GRS 1915+ 105 (R00). The values of the positive time lags for this source are consistent with the BH mass being around 20 solar masses (see BOR 99 for the BH mass determination in GRS 1915+ 105). We show that the absolute value of the time (phase) lags get higher with the energy. In fact, Wijands et al. (1999) for XTE J1550-564 (see also Remillard et al. 2001) and Tomick & Kaaret (2000) for GRS 1915+ 105 show that the phase lags of both signs increase from 0 to 0.5 radians as the photon energy varies from 3 keV to 100 keV. These phase lag changes correspond to the time lag changes from 0 to 15 m s and from 0 to 50 m s for XTE J1550-564 and GRS 1915+ 105 respectively. These values are very close to what we obtain in our simulations.

For  $\tau_1 > 15$  m s we get the time lags of both signs. Positive values of  $\tau$  should be of order 30 m s and higher. Negative values should not be higher than 20 m s for a 10 solar mass BH. Our simulations demonstrate that for high accretion rates time lags of both signs are present, i.e. the upscattering and down-scattering are equally important in the formation of CI spectrum, whereas for the low mass accretion rates the upscattering process leads to the CI spectral formation and only the positive times lags are present. Our simulations are in a good agreement with the R00's values of  $\tau = 30 - 60$  m s. The results for the simulated time lags can be understood using the simple upscattering model (see ETC). We assume that at any scattering event the relative mean energy change is constant, i.e.  $\Delta E/E = \langle \Delta E \rangle / E$ . The number of scatterings  $k$  which are needed for the soft photon of energy  $E_0$  to gain energy  $E$  is  $k(E) = \ln(E/E_0) = \ln(1 + \Delta E/E)$ . Then  $\tau = k \cdot l(1 - \beta^2)^{-1/2} = c$  where  $l$  is the photon mean free path,  $l = [p(E) \cdot n]^{-1}$ ,  $(1 - \beta^2)^{-1/2}$  is the relativistic dilatation factor (e.g. Landau &

Lifshitz 1971) and  $b(E)$  is an energy dependent factor less than unity (e.g. Pozdnyakov et al, 1983). The free path  $l$  is estimated as  $l = 2(r=r_g)^{1.5} r_g = b(E) \underline{m}$  with an assumption that the number density  $n$  is calculated for the free fall distribution, (see LT 99, Eq. 2). With  $r=r_g = 1.18$  (see Fig. 2, curve d),  $\underline{m} = 4$  and  $b = 0.5$  for  $E = 100$  keV we get  $l = 1.2 r_g b(E) = 1$  for  $E = 10$  keV and  $r=r_g > 2$  and consequently  $l > 1.5 r_g$ .<sup>8</sup>

## 5. Summary and Conclusions

Using Monte Carlo simulations we have presented a detailed timing analysis of the X-ray radiation from a CI atmosphere. (1) We confirm TZ98's results that the high energy photons are produced predominantly in the deep layers of the CI atmosphere from 1 to 2 Schwarzschild radii. (2) We also confirm that the 100-Hz phenomena should be seen in the high energy tail of the spectrum rather than in the soft spectral component because the inner part of the converging inflow is mostly fed by soft photons from the innermost part of the disk but the contribution of this disk area to the disk emission is small. (3) We find that the characteristic time lags in the converging inflow are order of a few tens of ms at 10 keV and the hard (positive) time lags increase logarithmically with energy. (4) We demonstrate that soft (negative) along with hard (positive) lags are present in the X-ray emission from the converging inflow for the mass accretion higher than Eddington. In the end we can also conclude that that almost all of the X-ray timing and spectral properties of the high-soft state in BHs tends to indicate that the high energy tail of spectrum is produced within the CI region, (1–3) where the bulk inflow (gravitational attraction) is a dominant process.

We acknowledge the fruitful discussions with Chris Shrader and Paul Ray. We also acknowledge the useful suggestions and the valuable corrections by the referee which improve the paper presentation.

---

<sup>8</sup> It is worth noting that the emergent high energy photon gains its energy being predominantly close to horizon,  $r = (1–2)r_g$  where the photon trajectory are close to circular (e.g. TZ98). Thus our estimated values of the free path  $l = (1–1.5)r_g$  are consistent with the trajectory length. With  $\tau = 0.1$  extracted from our simulations for  $E < 100$  keV where the extended power law is seen in the spectrum (see also Papathanassiou & Paltis 2001, Fig. 3) the time lags are  $\tau = 7.6$  ms and 50 ms for  $E = 10$  keV and 100 keV respectively.

## REFERENCES

- Borozdin, K ., Revnivtsev, M ., Trudolyubov, S ., Shrader, C . & Titarchuk, L . 1999, ApJ, 517, 367 (BOR 99)
- Chakrabarti, S K ., & Titarchuk, L . G . 1995, ApJ, 455, 623
- Chandrasekhar, S . 1960, Radiative Transfer, New York: Dover
- Cui, W ., Zhang, S N . & Chen, W . 2000, ApJ, 531, L45
- DiSalvo, T ., et al. 2000, ApJ, 544, L119
- Ebisawa, K ., Titarchuk, L . & Chakrabarti, S K . 1996, PASJ , 48, 59 (ETC )
- Iaria, R ., Burderi, L ., DiSalvo, T ., La Barbera, A . & Robba, N R . 2001, ApJ, 547, 412
- Landau, L D . & Lifshitz, E M . 1971, The Classical Theory of Fields , New York: Pergamon Press
- Laurent, P ., & Titarchuk, L . 1999, ApJ, 511, 289 (LT 99)
- Lehr, D E ., Wagoner, R V . & Wilms, J . 2000, astro-ph/0004211
- Nobili, L ., Turrota, R ., Zampieri, L ., & Belloni, T . 2000, ApJ, 538, L137
- Nowak, M A ., Wilms, J ., Heindl, W A ., Pottschmidt, K ., Dove, J B . & Begelman, M C . 2001, MNRAS, 320, 316
- Papathanassiou, H . & Saltis, D . 2001, MNRAS, in press, astro-ph/0011447
- Pozdnyakov, L A ., Sobol', I M . & Sunyaev R A . 1983, Astrophys. Space. Phys. Rev., 9, 1
- Rees, M . 1997, Phys. Scr., 17, 193
- Reig, P ., Kylas, N D . & Spruit, E C . 2001, A & A , 375, 155
- Reig, P ., Belloni, T ., van der Klis, M ., Mendez, M ., Kylas, N D . & Ford, E C . 2000, ApJ, 541, 883 (R 00)
- Remillard, R . A ., Sobczak, G . J ., Munro, M P ., & McClintock J E . 2001, ApJ, in press astro-ph/0105508
- Skibo, J G ., & Demmer, C D . 1995, ApJ, 455, L27
- Shrader, C R ., & Titarchuk, L . G . 1998, ApJ, 499, L31



Strickman, M., & Barret, D. 1999, in proceedings of the 4th Compton Symposium (eds. M. L. McConnell & J. M. Ryan) p. 222

Titarchuk, L., & Shrader, C. 2002, ApJ, in press

Titarchuk, L., Mastichiadis, A., & Kylas, N. D. 1997, ApJ, 487, 834

Titarchuk, L., & Zannias, T. 1998, ApJ, 493, 863 (TZ98)

Tomasko, J. A., & Kaaret, P. 2000, ApJ, 548, 401

Wijnands, A. D., Homan, J., & van der Klis, M. 1999, ApJ, 526, L33

# HIGH STATE OF BLACK HOLE SYSTEM

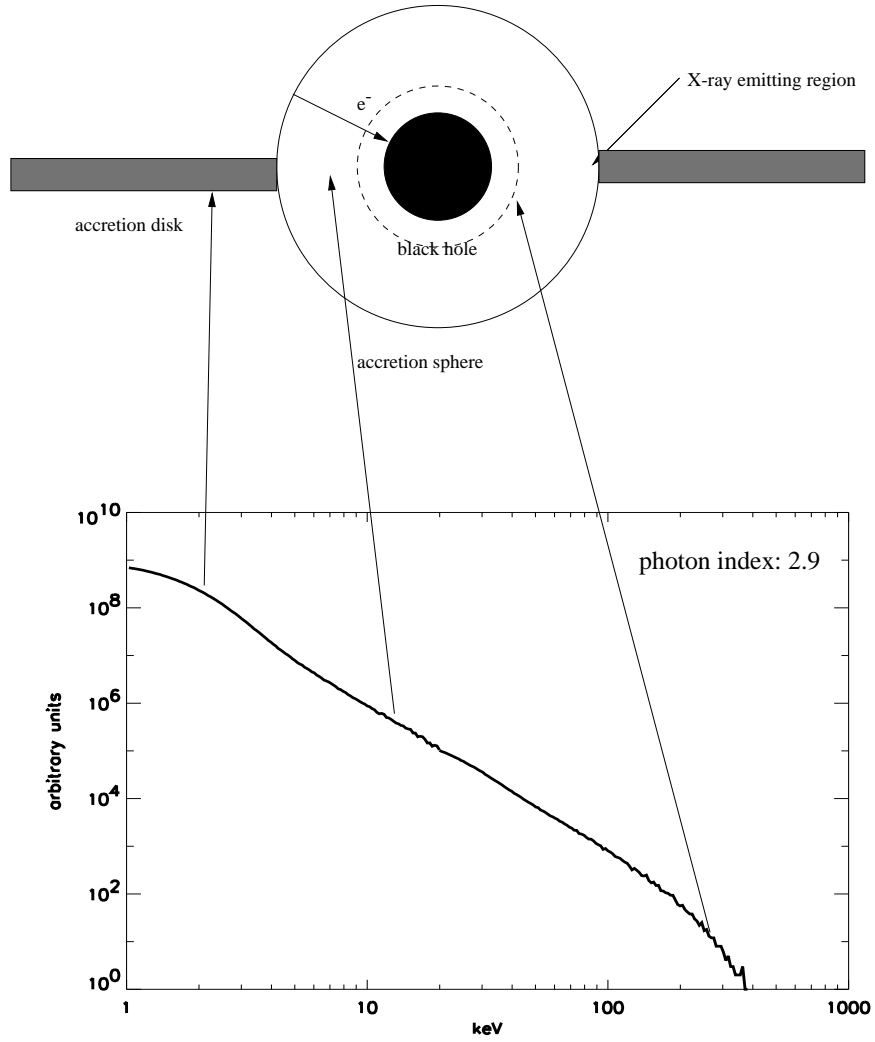


Fig. 1. | Monte Carlo simulated emergent spectrum of Converging Inflow. Mass accretion rate in Eddington units,  $\dot{m} = 4$ , electron temperature of the inflow  $kT_e = 5$  keV.

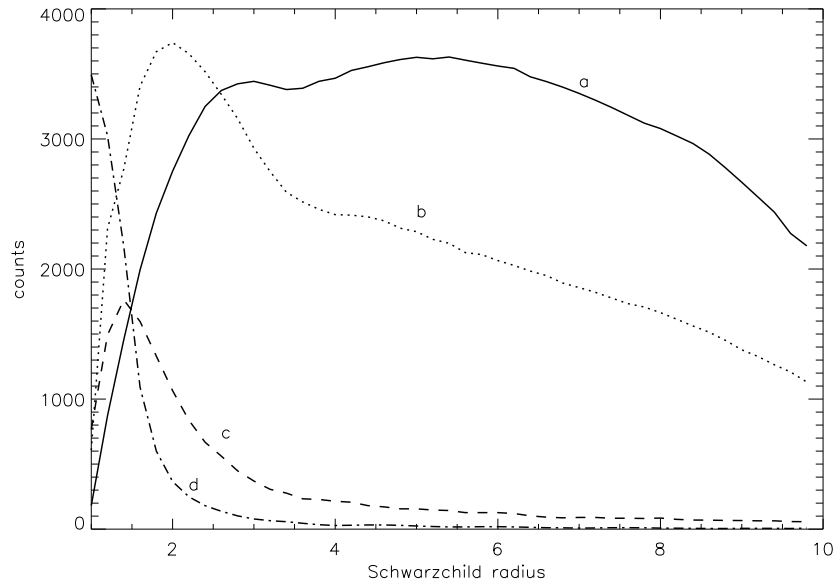


Fig. 2. Source photon spatial distribution in the converging inflow atmosphere for different energy bands: a is for (2-5) keV, b is for (5-13) keV, c is for (19-29) keV and d is for (60-150) keV.

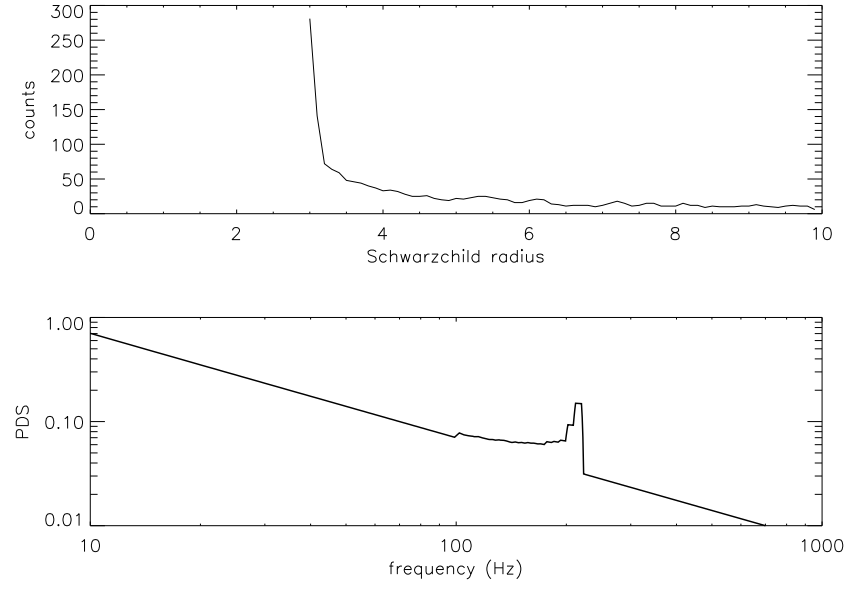


Fig. 3. | Distribution of soft photons over disk radius which upscatter to energies 10 keV and higher in CI atmosphere (upper panel). Power density spectrum for photon energies higher than 10 keV (lower panel). It is assumed that any disk annulus oscillates with Keplerian frequency. The continuum is a red noise.

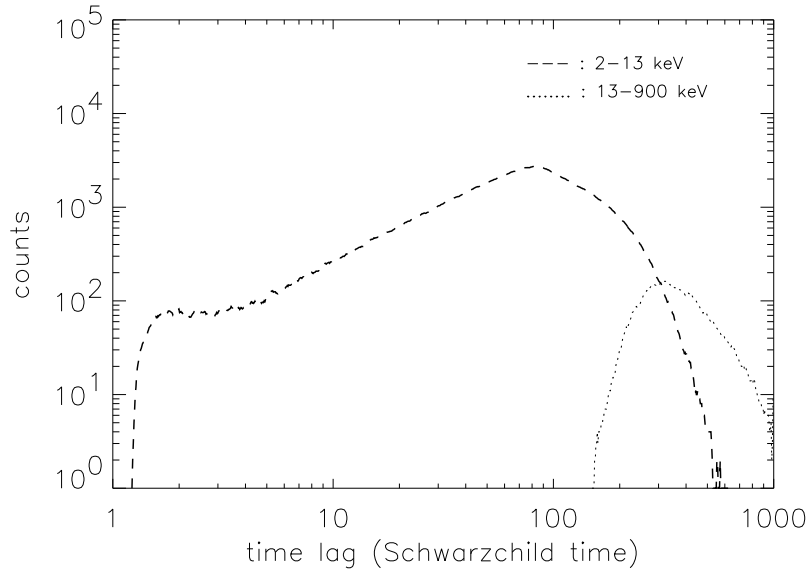


Fig. 4. | Time lag distributions for two energy bands. One can clearly see the area between 150 and 600  $r_s=c$  where time lags of both signs can be present.